第 I 部門　Aerodynamic characteristics of cable with spiral protuberances in inclined condition

Kyoto Univ.	Student M.	○Tung Quang Do	Kyoto Univ.	Member	Tomomi Yagi
Kyoto Univ.	Student M.	Takuya Shimoda	Kyoto Univ.	Student M.	Haruki Fukushima
Kyoto Univ.		Thu Minh Dao	Kyoto Univ.	Member	Kyohei Noguchi

1. Introduction

Cable with 12 spiral protuberances and 27° winding angle has been introduced as a solution to prevent rain-wind induced vibration of cable-stayed bridge[1)]. However, there are still unknown aerodynamic properties of this cable. For example, helical wire under the inclined condition generate lift force to induce buffeting, which has similar properties with cable with spiral protuberances[2)]. Also, there is a possibility that dry state galloping occurs because of the drag crisis. In this research, by conducting the static force measurement using a wind tunnel, the characteristics of cable with spiral protuberances are investigated. The results are utilized to examine the dry galloping and buffeting characteristics under the inclined condition.

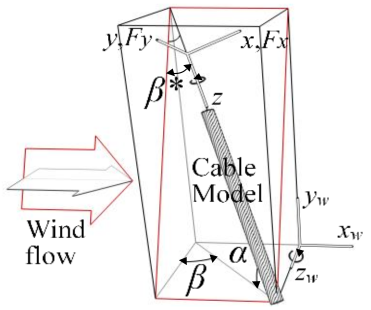

$\beta^* = \sin^{-1}(\cos\alpha \cdot \sin\beta)$

Fig. 1. Definition of β^*

2. Static force measurement of cable with spiral protuberances

The detail of yawed α[°], inclined β[°], relative angle β^* [°] is shown in Figure 1. In the uniform flows, wind forces defined by wind axis is independent from α. Therefore, in this research, α was kept 0° while β was changed from 0° to 45° with an interval of 5°. Static force measurement was conducted for both circular cable and cable with spiral protuberances. The drag and lift force coefficients (C_D and C_L) were obtained by Eq. (1). where ρ: air density [kg/m^3], U: wind velocity [m/s], D: cable diameter [m], F_D and F_L: drag and lift force acting on the cable, L: cable length [m].

$$C_D = \frac{F_D}{\frac{1}{2}\rho U^2 DL}, \quad C_L = \frac{F_L}{\frac{1}{2}\rho U^2 DL} \qquad (1)$$

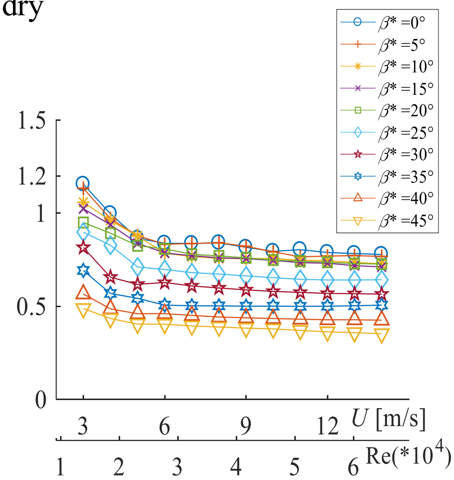

Fig. 2. Drag force coefficient

For the cable with spiral protuberances, Fig. 2 shows C_D - Reynold number (Re) relationship. Drag crisis region is observed when Re is smaller than around 2.5×10^4. C_D of cable with spiral protuberances when $\beta^* = 0°$ was smaller than 1.2 which is common for circular cable. The result for super critical Re, which is located outside drag crisis region, corresponds to the previous research[1)]. Dry galloping characteristics should be examined because of drag crisis. Fig. 3 shows C_L increases when β^* increases which agreed with past research[2)]. Because of surface configuration when cable is inclined, the time average flow fields are different between upward and downward surface. Thus, lift force is non-zero. To eliminate the lift force for the whole cable span, the winding angle direction of spiral protuberances can be reserved alternatively.

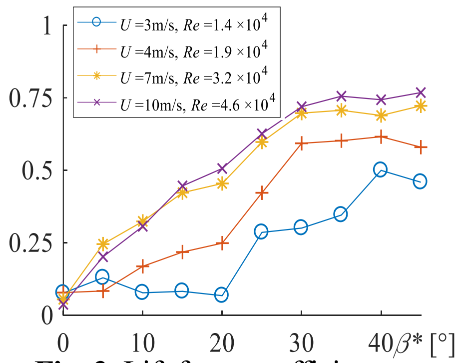

Fig. 3. Lift force coefficient

Tung Quang DO, Tomomi YAGI, Takuya SHIMODA, Haruki FUKUSHIMA, Thu Minh DAO and Kyohei NOGUCHI
do.tung.48z@st.kyoto-u.ac.jp

3. Dry galloping characteristic of cable with spiral protuberances

Eq. (2) was derived to calculate aerodynamic damping ratio ξ_a using the quasi-steady theory for dry galloping to judge whether dry galloping occurs[3]. $\xi_a > 0$ suggests that cable is stable against galloping.

$$\xi_a=\frac{\mu \mathrm{Re}}{4m\omega_n}\cos\theta_v\left\{\cos\theta_v\left[C_D\left(2\cos\beta^*+\frac{\tan^2\theta_v}{\cos\beta^*}\right)+\frac{\partial C_D}{\partial \mathrm{Re}}\mathrm{Re}\cos\beta^*+\frac{\partial C_D}{\partial \beta^*}\mathrm{Re}\sin\beta^*\right]-\sin\theta_v\left[C_L\left(2\cos\beta^*-\frac{1}{\cos\beta^*}\right)+\frac{\partial C_L}{\partial \mathrm{Re}}\mathrm{Re}\cos\beta^*+\frac{\partial C_L}{\partial \beta^*}\mathrm{Re}\sin\beta^*\right]\right\} \quad (2)$$

where μ : dynamic viscosity of air, θ_v [°] : angle between cable-wind plane and the moving cable velocity direction, ω_n [rad/s] : angular frequency of the structure. Fig. 4 shows ξ_a at $\beta^* = 45°$ for cable with spiral protuberances. Lift force caused the asymmetric contour of ξ_a against $\theta_v = 90°$ and the decrease of ξ_a under the drag-crisis region. Since ξ_a is positive for the Re belongs to both inside and outside drag crisis regions. Thus, dry galloping will not occur for cable with spiral protuberances.

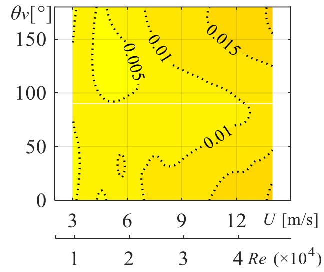

Fig. 4. ξ_a at β^*=45°

4. Buffeting characteristic of cable with spiral protuberances

Kikuchi[2] showed that lift force might induce buffeting on inclined helical wire. Thus, equation of motion containing buffeting terms is newly introduced, which is shown by Eq. (3).

$$\begin{cases} m\ddot{x}+c\dot{x}+kx=\frac{1}{2}\rho\left(C_D(\hat{\beta}_r,U_r)\cos\theta+C_L(\hat{\beta}_r,U_r)\sin\theta\right)DU^2\left(1-\frac{2}{U}\dot{x}\cos\hat{\beta}\right) \\ m\ddot{y}+c\dot{y}+ky=\frac{1}{2}\rho\left(-C_D(\hat{\beta}_r,U_r)\sin\theta+C_L(\hat{\beta}_r,U_r)\cos\theta\right)DU^2\left(1-\frac{2}{U}\dot{x}\cos\hat{\beta}\right) \end{cases} \quad (3)$$

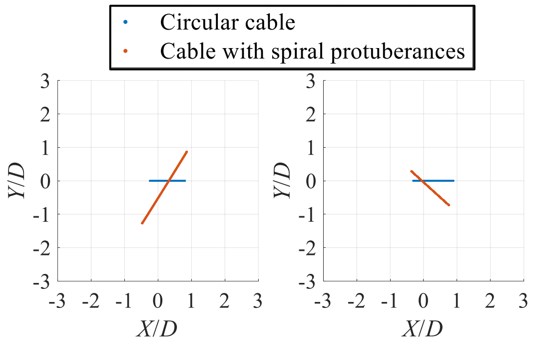

a. U = 7m/s, $\hat{\beta}(t)$ = 30°+10°sin(2πft)

b. $U(t)$ = 7+ 0.5sin(2πft) m/s, $\hat{\beta}$ = 30°

Fig. 5. Trajectory motion of the cable

where m: mass of cable per unit length [kg/m], $\hat{\beta}_r$ and U_r : relative wind flow angle and relative wind velocity due to the self-motion of cable, θ : relative angle of attack (Angle between relative wind onto structure axis). To evaluate the validity of the proposed equations, two examples of time-varying components $\hat{\beta}(t)$ and $U(t)$ are given virtually. The buffeting responses of inclined cable is observed by the time history analysis solving Eq. (3). Fig. 5 shows the buffeting response when $\hat{\beta}(t)$ or $U(t)$ fluctuates with the same frequency as the natural frequency f of cable. Vertical vibration occurs for the cable with spiral protuberances in the simulation. Fig. 5a shows that amplitude of cable with spiral protuberances is larger than that of circular cable. However, the vibration in Fig. 5a hardly occur for an actual cable-stayed bridge since out plane deformation of cable does not exist in actual cable-stayed bridge. Therefore, buffeting is not significant in cable stabilities. Fig. 5b shows that horizontal amplitude of cable with spiral protuberances is smaller than that of circular cable. Vertical amplitude can be eliminated by using the countermeasure as mentioned in section 2. Therefore, cable with spiral protuberances is stable against buffeting.

5. Conclusion

1) In the case of cable with 12 spiral protuberances and 27° winding angle, drag crisis is observed when Reynold number is smaller than around 2.5 × 10^4. 2) The lift force appeared for cable with spiral protuberances under the inclined condition. However, drag force become smaller than circular cable. 3) Cable with spiral protuberances is stable against dry galloping even in the drag crisis region. 4) Vertical vibration due to buffeting is observed for cable with spiral protuberance because of lift force when $\hat{\beta}(t)$ and $U(t)$ are virtually set, while cable with spiral protuberances is stable against buffeting in actual cable-stayed bridge.

References 1) Yagi et al.: Modification of surface configurations of stay cables for drag force reduction and aerodynamic stabilization, Proc., 13th International Conference on Wind Engineering, 2011. 2) 菊池：ヘリカルロッド巻き電線に生じた振動の観測結果と揚力抗力の影響，第 25 回風工学シンポジウム論文集，2018. 3) Macdonald and Larose: A unified approach to aerodynamic damping and drag/lift instabilities, and its application to dry inclined cable galloping, Journal of Fluids and Structures, 22(2), 229-252, 2006.